2018-02-24

An improved model for the ikaite-glendonite transformation: evidence from the Lower Cretaceous of Spitsbergen, Svalbard

Vickers, M

10.17850/njg98-1-01
NORWEGIAN JOURNAL OF GEOLOGY
Geological Society of Norway

An improved model for the ikaite-glendonite transformation: evidence from the Lower Cretaceous of Svalbard

Madeleine Vickers[1*], Matthew Watkinson[1], Gregory D. Price[1], Rhodri Jerrett[2]
[1] Plymouth University, Plymouth, United Kingdom
*madeleine.vickers@plymouth.ac.uk
[2]School of Atmospheric, Earth and Environmental Sciences, Manchester University, Manchester, United Kingdom

Abstract

Glendonites, pseudomorphs after marine sedimentary ikaite, are found throughout the Lower Cretaceous succession of Svalbard. Existing models for the ikaite-to-glendonite formation do not explain the different petrological fabrics observed in the glendonites of Lower Cretaceous Svalbard. This study presents an improved model for the formation of these glendonites, based on petrographic and geochemical observations, and published work on ikaite breakdown (e.g. Tang et al., 2009). We show that for the glendonites of lower Cretaceous Svalbard, methane is unlikely to be the sole or indeed main driver behind their formation, and present an improved model for their formation that accounts for the varied petrographic fabrics observed in these particular glendonites. Coupled with our new model, stable isotope data demonstrate why bulk samples of ancient glendonite cannot be used for palaeotemperature reconstructions.

Keywords
Palaeoclimate; early diagenesis; glendonite; Early Cretaceous

1. Introduction

Glendonites are calcite pseudomorphs after the mineral ikaite, a metastable, hydrated form of calcium carbonate ($CaCO_3.6H_2O$). Unlike other $CaCO_3$ polymorphs, ikaite becomes more stable with decreasing temperatures (e.g. Marland; 1975; Bischoff et al., 1993; de Lurio and Frakes, 1999), and for this reason the presence of glendonites in sedimentary rocks has been used to infer palaeo-cold water conditions (e.g. Selleck et al., 2007; Frank et al., 2008a,b; de Lurio and Frakes, 1999; Price and Nunn, 2010; Grasby et al., 2017). Ikaite requires specific chemical conditions to become metastable. This includes elevated alkalinity and phosphate concentrations (to inhibit calcite and aragonite growth), and low temperatures (<8°C; Bischoff et al., 1993; Buchardt et al., 2001; Suess et al., 1982; Swainson and Hammond, 2001; Zhou et al., 2015). Furthermore, the experiments of Hu et al. (2014) with artificial seawater found that pH and salinity may also exert a strong control over ikaite precipitation.

Ikaite was first identified growing in tufa towers in the Ikka Fjord by Pauly (1963). Here, conditions for ikaite growth have been met due to highly alkaline spring water mixing with sea water (Buchardt et al., 2001). Ikaite has since been found growing in other environments where temperature, pressure and chemical conditions are suitable to stabilise ikaite and inhibit calcite/aragonite growth, including on Arctic and Antarctic sea ice; the carapaces of frozen shrimp (Mikkelsen et al., 1999; Dieckmann et al., 2008, 2010); and more commonly, growing below the sediment-water interface in modern shelf settings (e.g. Lu et al., 2012; Schubert et al., 1997; Suess et al., 1982; Zhou et al., 2015). It is this marine sedimentary ikaite that pseudomorphs into the stellate calcite nodules now known as “glendonites” (after those found in the Permian deposits of

Glendon, New South Wales, Dana, 1849; David et al., 1905), which are found repeatedly in the sedimentary record, including in the Lower Cretaceous succession of Svalbard (Maher et al., 2004; Price and Nunn, 2010; Vickers et al., 2016).

Marine sedimentary ikaite is found in modern shelf settings between c. 3 and 20 m below the sediment-water interface, around the sulphate-methane transition (Lu et al., 2012; Schubert et al., 1997), where pore-water temperatures are < 8 °C (Zhou et al., 2015). Two biogeochemical processes may provide the carbon source and specific chemical conditions necessary for marine sedimentary ikaite formation: (1) organic matter breakdown by sulphate reduction (Suess, 1982), and (2) oxidation of methane during sulphate reduction (Rickaby et al., 2006; Schubert et al., 1997; Teichert and Luppold, 2013; Morales et al., 2017). Possible methane sources include methanogenesis (anaerobic bacterial organic-matter breakdown) or the decomposition of solid methane hydrates (Schubert et al., 1997; Morales et al., 2017). The methane is believed to diffuse from a deeper source up through the sedimentary pile until it becomes oxidised at a redox barrier (Schubert et al., 1997; Greinert and Derkachev, 2004; Morales et al., 2017). Both methane oxidation and organic matter breakdown occur in the sulphate reduction zone and result in the high carbonate alkalinity and high phosphate concentrations required for ikaite growth. Some authors imply that the oxidation of methane from methane seeps via methanotrophic bacteria creates such favourable environments for glendonite formation that temperatures may have been elevated above the typical < 8 °C (e.g. Teichert and Luppold, 2013; Morales et al., 2017), and therefore the presence of glendonites in sedimentary successions are more useful as palaeo-methane seep indicators. As the $\delta^{13}C$ value of ikaite reflects the $\delta^{13}C_{DIC}$ of the porewater carbon pool from which it grew (e.g. Lu et al., 2012; Teichert and Luppold, 2013), methane-derived ikaite can be distinguished from that which had organic matter as its main carbon source.

There is much uncertainty about the ikaite-to-glendonite transformation, as the petrology of glendonite in thin section suggests multiple phases of diagenetic growth, and the drivers behind these are debated (Swainson and Hammond, 2001; Greinert and Derkachev, 2004; Huggett et al., 2005; Selleck et al., 2007; Frank et al., 2008a,b; Teichert and Luppold, 2013; Morales et al., 2017). This study sets out to assess whether this existing model for ikaite-to-glendonite transformation fits with the petrological and geochemical observations of the glendonites of Svalbard, and to improve or re-model this transformation according to these observations. Our model accounts for petrographic differences observed between the Rurikfjellet Formation and Carolinefjellet Formation glendonites, and highlights the potential pitfalls of using glendonites quantitative palaeothermometric reconstructions. The results of this study have implications for the understanding of early diagenetic processes occurring below the sediment-water interface in the marine realm; informing the current understanding of regional-to-global geochemical and/or temperature trends in the Early Cretaceous.

1.1 Geological setting

During the Early Cretaceous Spitsbergen was located at c. 65 °N and was part of a shallow epicontinental sea (Fig. 1a). Glendonites are found in the Lower Cretaceous of Svalbard, in the Hauterivian – Barremian-aged Kikutodden Member of the Rurikfjellet Formation (Price and Nunn, 2010; Vickers et al., 2016) and upper Aptian – lower Albian of the Carolinefjellet Formation (upper Dalkjegla and Innkjegla members; Maher et al., 2004; Vickers et al., 2016). The Rurikfjellet Formation represents a regressive succession, moving from (oxic) open marine shelf environments in the lower Wimanfjellet Member to shallow marine shelf deposits of the Kikutodden Member

(Mørk et al., 1999; Vickers, 2017). The Kikutodden Member, which contains the glendonites, consists of coarsening up packages consisting of shale, mudstone, siltstone and sandstone, with siderite concretions common in the shale facies (e.g. Midtkandal et al., 2008; Vickers et al., 2016). The Carolinefjellet Formation was also deposited in open marine shelf conditions (e.g. Grundvåg and Olaussen, 2017), and the glendonites are found in both the sand-rich Dalkjegla Member and shale-dominated, carbonate-concretion-bearing Innkjegla Member (e.g. Krajewsky and Luks, 2003; Maher et al., 2004; Vickers et al., 2016). Glendonites were collected for this study from two sites on Spitsbergen; Festningen (Fig. 1b; 78°09.98'N, 13°94.32'E), located on the southwestern side of Isfjorden; and the succession outcropping along the road between Longyearbyen airport and Longyearbyen itself (Fig. 1c).

2. Methods

Careful bed-by-bed searches for glendonites were made in the studied outcrops at Festningen and around Adventdalen (Fig. 1b and c). The locations of glendonite horizons were recorded via high-resolution conventional graphic logging, and whole glendonites were sampled from each glendonite horizon. Conventional facies analysis was undertaken to constrain the environment of deposition of the glendonite bearing horizons (see supplementary material).

Carbon and oxygen isotope analysis of the bulk glendonites was performed at Plymouth University using an Isoprime isotope ratio mass-spectrometer using ~0.5 mg of powdered sample. Carbon and oxygen isotope ratios are expressed in standard delta notation as per mil deviation from the Vienna Pee Dee Belemnite (VPDB) standard. Measured results were calibrated against USGS standards (NBS19, CO8 and CO9).

Polished thin sections were examined using a polarising light microscope, and cathodoluminescence (CL) petrography was performed using a CL8200 Mk5-2 Optical CL System, operating at an accelerating voltage of ≤ 25 kV and current of ≤ 400 – 500 μA. Selected thin sections were examined using a JEOL 7001 FESEM at Plymouth University Electron Microscopy Centre at 20kV with a working of 10mm using the backscatter electron detector. Point analyses, element maps and line transects were collected using an Oxford Instruments AZtecEnergy energy dispersive X-ray analysis system.

3. Results

3.1 Sedimentary and stratigraphic location of glendonite horizons

Altogether, 8 glendonite horizons were identified in the Festningen section, and 2 horizons identified in the outcrop by the Airport road in the Adventdalen region (Fig. 2 and Table 1).
In the Festningen section, 3 glendonite horizons were found in the Kikutodden Member of the Rurikfjellet Formation, at 409 m, 411 m and 441 m. Glendonites of the Carolinefjellet Formation were found in 6 horizons between 655 and 753.15 m at Festningen, and lower down in the succession at the Airport road Section near Longyearbyen (at 2.5 m and 118 – 199 m). This correlates to c. 602 m in the Festningen section. The glendonites were found in sandstone or siltstone, all in fully marine facies associations, ranging from proximal offshore transition zone through to (proximal) open marine shelf (Table 1; see supplementary material for a summary of the facies analysis). The depositional environment for the glendonites, all below fair weather wave

base, sometimes ranging to just below storm wave base, constrains the minimum depth of glendonite formation to below that of storm wave base, which is on the scale of tens of metres.

3.2 $\delta^{13}C$ and $\delta^{18}O$ analysis

For the bulk glendonite data the minimum $\delta^{13}C$ value was -30.9 ‰ for APT2.2c, and the maximum $\delta^{13}C$ value was -13.3 ‰ for FST753.15 (Fig. 3A). The maximum $\delta^{18}O$ value was -12.3 ‰ for FST411.2, and the minimum $\delta^{18}O$ value was -1.0 for APT2.2c (Fig. 3B). The $\delta^{18}O$ and $\delta^{13}C$ data show a negative correlation (Fig. 3C). The glendonites from the Rurikfjellet Formation (Hauterivian – Barremian aged) show a wider spread in $\delta^{18}O$ values than those from the Late Aptian Carolinefjellet Formation (Fig. 3B); from -12.3 to -2.8 ‰ (range of 9.5 ‰; mean of -8.8 ‰) vs -7.6 to -1.0 ‰ (range of 6.6 ‰, mean of -5.7 ‰).

3.3 Shape

The glendonites collected may be grouped according to their physical shape, although it is noted that all reflect single or combinations of the bipyramidal, elongate ikaite crystal shape (e.g. Schubert et al., 1997; Suess, 1982; Lennie et al., 2004; Rickaby et al., 2006; Lu et al., 2012; Hu et al., 2014). The glendonites collected from the Lower Cretaceous of Spitsbergen tend to be rosette in form (composed of many intersecting blades; Table 1 and Fig. 4 A, H and K). These rosettes may be slightly flattened (Fig. 4 D), or may be found inside carbonate concretions (e.g. Fig. 4 G and H), where they may be cylindrical (Fig. 4 G). In some horizons, the glendonites were larger and broke into pieces during collection (broken aggregates of radiating blades, described in Table 1 as “partial rosette”; Fig. 4 B,C,E). They appear to have broken from the centre outwards (half-blades; no full blades preserved). Some glendonites appear as single or double blades (Fig. 4 I and J).

3.4 Internal structure

The glendonites show a range of internal structures, from (a) mm-scale zoning on each blade of calcite (hearafter referred to as macro-zoned; Fig. 5 A, B); (b) core or rim evident but otherwise no apparent zones (Fig. 5 C, D); or (c) homogeneous across centre to edge of glendonite (hereafter referred to as unzoned; Fig. 5 E, F). Under light-microscope, CL and SEM, the micro-structure can be seen (Fig. 6). In addition to calcite, pyrite is observed, and some show areas of siliceous silt inclusion. Different calcite phases are evident, interpreted as representing different generations of calcite (also identified in glendonites from a variety of locations by Huggett et al., 2005; Teichert and Luppold, 2013; Larsen, 1994; David et al., 1905; Boggs, 1972; McLachlan et al., 2001; Selleck et al., 2007; Fig. 6). The different calcite phases (types) are described below:

Type I: small, sub-rounded to lath-shaped light brown to grey (due to inclusions) calcite crystals. These are frequently zoned or with clear rim/core, and may have an irregular outline. Type I calcite is often inclusion-rich, particularly in the cores. Brightly luminescent (non-ferroan) with non-luminescent zones (ferroan).

Type II: brown calcite, zoned. Grows from the surface of Type I grains. May be lobate/botryoidal. Less luminescent than Type I, suggesting higher overall iron content. Alternates between thin zones of luminescence and non-luminescence, evidence of increasing iron enrichment towards outer edge. Frequently the boundary between type II and III calcite appears etched.

Type III: brown or transparent calcite spar; mostly ferroan (non-luminescent); infilling.

4. Discussion

4.1 Sedimentological context

The depositional environment for both the Kikutodden Member and Carolinefjellet Formation is composed of fully marine, proximal offshore transition zone through to open marine shelf fully marine shelf facies associations (Fig. 2). This is consistent with the location of modern marine sedimentary ikaite, which is found in marine shelf environments in the high latitudes (e.g. Antarctic Peninsula, Laptev Sea continental margin; Schubert et al., 1997; Suess et al., 1982; Zhou et al., 2015). The observations that the sediments surrounding the glendonites are deformed around the pseudomorphs (e.g. Fig. 4 D; also observed by Selleck et al., 2007; Frank et al., 2008a,b; Huggett et al., 2005; Greinert and Derkachev, 2004), and the occurrence of glendonites in horizons with cannon-ball concretions (and, occasionally inside concretions, Fig. 4 G and H), suggests that the ikaite transformed to glendonite whilst the sediment was uncompacted and still in the sulphate reduction zone (where it is believed the ikaite grew; Suess, 1982; Rickaby et al., 2006; Schubert et al., 1997; Teichert and Luppold, 2013). This is consistent with Krajewski and Luks (2003) who also suggest that the cannon-ball carbonate concretions in the Innkjegla Member of the Carolinefjellet Formation, Svalbard, formed in the upper part of the sulphate reduction zone, where the bacterial oxidation of organic matter provides the carbon source for calcite precipitation.

The key difference between the Carolinefjellet and Kikutodden Member glendonite horizons is that sedimentation rates appear to be much higher in the Carolinefjellet Formation than in the Kikutodden Member. This is suggested by both the improved chemostratigraphy of Vickers et al. (2016) for the Kikutodden Member, and the fact that more intense bioturbation, more fossil material and carbonate concretions occur in the Kikutodden Member than the Carolinefjellet Formation (Figure 4). The lower sedimentation rates in Kikutodden Member means that the sediments were kept in shallow diagenetic zones for longer than those of the Carolinefjellet Formation.

4.2 Petrology

There are notable petrological differences between the glendonites from the upper part of the Kikutodden Member and those of the Carolinefjellet Formation, which may be indicative of different conditions prevailing during ikaite growth and transformation to glendonite. The glendonites of the Rurikfjellet Formation show macro-zoning, whereas those in the Carolinefjellet Formation are unzoned or show distinct cores.

All glendonites collected in this study preserve at least three calcite phases. The majority of existing studies on glendonites also show at least 3 phases of calcite growth (Teichert and Luppold, 2013; David et al., 1905; Boggs, 1972; Larsen, 1994; McLachlan et al., 2001; Huggett et al., 2005; Selleck et al., 2007). Type I calcite, as described in previous studies, is interpreted to represent the original ikaite-derived calcite (e.g. Larsen, 1994; Frank et al., 2008a,b; Huggett et al., 2005; Teichert and Luppold, 2013). This primary ikaite-derived calcite is described in well-preserved glendonites from around the globe (e.g. Australia, North America, Siberia; Japan, Denmark, U.K.; Larsen, 1994; Greinert and Derkachev, 2004; Huggett et al., 2005; Selleck et al., 2007; Frank et al., 2008a,b; Teichert and Luppold, 2013). Type I calcite makes up ~31% by volume of the pseudomorph (since in ikaite, 69% volume of the structure is water, which is lost when ikaite transforms to calcite, resulting in a 2/3rd volume loss; de Lurio and Frakes, 1999; Larsen, 1994). The botryoidal Type II calcite of this study is interpreted as forming after Type I and before Type III, based on the

boundary relationships observed in thin section examination. Intermediate phases of diagenetic calcite described from glendonites in other studies may show similar microscopic concentric zoning, and are described as spherulitic by Huggett et al. (2005) and Frank et al. (2008a,b). Other forms of intermediate diagenetic (Type II) calcite have been described, including radiaxial- fibrous (Frank et al., 2008a,b); fibrous spherulitic (Huggett et al., 2005), forming syntaxial rims (Huggett et al., 2005); microsparitic to sparitic rims and euhedral rims (Greinert and Derkachev, 2004); and columnar infilling calcite (Teichert and Luppold, 2013), and it is likely that multiple phases of growth are encompassed by the term "Type II". Petrological and chemical observations in this study show that Type II calcite often shows increasing iron content outward, and has etched boundaries with Type III calcite, suggesting that the pore-water chemistry was changing as this secondary calcite precipitated, eventually becoming so acidic that dissolution, rather than precipitation, took place. The clear calcite spar observed in the glendonites of this study (Type III) is regarded as the final phase of diagenetic calcite growth (e.g. Teichert and Luppold, 2013; Selleck et al., 2007; Frank et al., 2008a,b; Huggett et al., 2005) as it is observed infilling the remaining porosity (see also Huggett et al., 2005; Kaplan, 1979), and is often Fe- and Mg- rich (this study; Huggett et al., 2005; Frank et al., 2008a,b; Teichert and Luppold, 2013), or even dolomitized (Huggett et al., 2005). This sparry calcite lacks the brown coloration seen in Type I calcite and secondary, Type II calcite phases.

The existing model for ikaite-glendonite transformation (e.g. as described by Teichert and Luppold, 2013, p.88) models ikaite transforming to calcite whereby the outer parts of the crystal transform before the centre of the crystal (i.e. the outer parts may be calcite which is growing diagenetic calcite rims whilst the centre remains stable). This model largely fits with observations of this study of the unzoned glendonites (and those showing distinctive cores and rims), although does not explain the observed etched boundaries on the Type II calcite (Fig. 6).

Coupled with the observations of increasing iron content outward in the Type II calcite (Fig. 6 B, D), and the fact that some glendonites are found inside carbonate concretions (a phenomenon also observed for glendonites from other locations (Teichert and Luppold, 2013; Huggett et al., 2005; Boggs, 1972); the presence of etched boundaries on less luminescent (increasingly iron-rich) Type II calcite is interpreted to be due to the sediments moving deeper into, then beyond, the sulphate reduction zone, under decreasing rates of sulphate reduction, as suggested by Krajewski and Luks (2003). The pyrite observed in the glendonites is likely to have formed whilst this local dissolution was occurring (Krajewski and Luks, 2003). This suggests that the secondary calcite (Type II) growth onto transformed- ikaite calcite (Type I) occurred soon after ikaite transformed to calcite, whilst the pseudomorphs were still in uncompacted sediments, and in the sulphate reduction zone.

It is observed in some studies that ikaite breaks down first to a mixture of vaterite (a metastable polymorph of $CaCO_3$, with the highest molar volume of the three anhydrous $CaCO_3$ polymorphs; e.g. Ito, 1998; Shaikh, 1990; Tang et al., 2009) and calcite. Tang et al. (2009) suggest that the vaterite is from solid state transformation of ikaite and the calcite is from dissolution of the ikaite and subsequent precipitation as calcite. No vaterite has been reported in glendonites, and it is unclear at what stage in the ikaite-to-glendonite transformation the vaterite transforms to calcite. Given the low stability of vaterite it can hence only be inferred that as ikaite destabilises it converts to vaterite + calcite + water (Fig. 7). Vaterite would then dissolve and re-precipitate as calcite (Type I calcite), the $CaCO_3$ source being the parent ikaite. Sometimes only the margins of the ikaite crystal destabilise, leaving a core of ikaite in the crystal centre (Fig. 7B). As observed in this study Type II calcite grows on the Type I calcite (Figs. 6 and 7). The $CaCO_3$ source for the Type II calcite is the pore

water in the sediments. Next, the core of ikaite destabilises to vaterite which the converts to calcite (Fig 9B). Cements continue to grow on the first generation of Type II calcite, and may begin to grow on the newly-formed Type I calcite in the core. As the sediments in which the pseudomorphs are sitting become progressively buried, they eventually pass out of the sulphate reduction zone. Conditions then become unfavourable for calcite precipitation and some etching of the existing calcite may occur (Fig. 7). Finally, an unknown length of time later, diagenetic sparry calcite (Type III) fills the remaining voids (Fig. 7).

For glendonites with distinct macro-zoning, it is hypothesised that conditions (thermal and chemical) oscillate around the ikaite stability field, resulting in the outside edge of the crystal becoming unstable while the rest of the crystal remains stable. The same processes occur whereby the ikaite progressively destabilises from the outside in, only at a slower rate than that which generated the glendonites with the distinct cores (Fig. 7C). Alternatively, it could be postulated that the crystal (ikaite or calcite) grew outward in progressive zones, as the fabric shows elements of both core-to-rim and rim-to-core growth. However, if the zoning occurred during ikaite growth, it is unlikely that it would be preserved after ikaite transformed, given the 2/3rd volume loss from the ikaite-to-calcite (via vaterite) transformation. If ikaite transformed to calcite, which then experienced slow zoned growth outward from the outer edge of the pseudomorph, the fabric in the centre of the crystals would be expected to show blebs of original "ikaite" calcite, which would not be seen in the zones as these grew after transformation. Given that the cores show the same structural elements as the rims, it is more parsimonious to conclude that the zoning must be due to the slow breakdown of ikaite from the outside in, with syn-transformational growth of secondary (Type II) calcite onto newly-formed calcite (Type I; e.g. Figs. 6 and 7). This agrees with the findings of Teichert and Luppold (2013), who conclude that the ikaite remains stable in the centre of the crystal for longer than in the margins.

It is hypothesised here that it is the rate and oscillatory nature of the chemical and thermal conditions that determine whether the crystal became zoned (very slow rate of transformation; oscillatory conditions; Fig. 7C), has a distinct core/rim (Fig. 7B), or shows no macro-zoning at all (Fig. 7A). This is supported by the observation that the macro-zoned glendonites are found in the more condensed Kikutodden Member of the Rurikfjellet Formation, where sedimentation rates were low, whereas the unzoned glendonites are found in the Carolinefjellet Formation, which is characterized by high sedimentation rates. Thus the glendonites of the Kikutodden Member sat for longer in the sulphate reduction zone, where chemical conditions appear to have oscillated between ikaite stability and instability, whereas those of the Carolinefjellet Formation were moved through sulphate reduction zone more rapidly and transformed wholly to calcite before secondary diagenetic calcite phases were precipitated.

4.3 Stable isotopes of glendonites

The $\delta^{13}C$ and $\delta^{18}O$ data show a strong negative correlation in both ancient glendonites and in cannonball concretions (e.g. Scotchman 1991; Krajewsky and Luks, 2004; Figs. 3 and 8). This is contrary to the positive trend seen in altered and pristine belemnite calcite, and calcite cement, whereby $\delta^{13}C$ is pushed to lighter values with time (e.g. typical meteoric diagenesis; Price and Nunn, 2010). This negative trend (Fig. 8) in glendonites and concretions reflects the evolution of the carbonate through the various paragenetic phases; later phases of carbonate growth show lighter $\delta^{18}O$ but heavier $\delta^{13}C$, reflecting the change in carbon source with depth from bacterial

organic matter breakdown in the sulphate reduction zone towards marine DIC sources (e.g. Frank et al., 2008; Selleck et al., 2007; Krajewsky and Luks, 2004; Scotchman, 1991). For Recent glendonites, which lack the later phases of diagenetic calcite, $\delta^{13}C$ values are within the range of organic matter to methane, whereas oxygen isotope values reflect a seawater or meteoric source (Fig. 8). Since bulk glendonites were used, it is noted that those showing heavier $\delta^{13}C$ and lighter $\delta^{18}O$ contain more (late-stage) sparry calcite, based on petrographic observations.

The glendonites of Spitsbergen show a broad range of $\delta^{13}C$ values, reflecting both variation in carbon source and proportion of later diagenetic calcite phases. The lowest $\delta^{13}C$ glendonite value is -30.9 ‰ and well within the range expected if methane was an important carbon source. However, the other glendonites analysed in this study do not show convincing methane $\delta^{13}C$ values, and, given the similarity in trends between cannon-ball concretion calcite phases and separated glendonite phases as evidenced in previous studies (Frank et al., 2008; Selleck et al., 2007; Krajewsky and Luks, 2004; Scotchman, 1991), we argue that methane is not necessary as a driver of glendonite formation. No carbonates were found showing the highly positive "residual" $\delta^{13}C$ values after microbial methanogenesis (e.g. a $\delta^{13}C$ range of + 1 to + 15 ‰, Irwin et al., 1977; Morales et al., 2017). Our interpretation of a mixed source of carbon is further supported by the fact that Recent transformed ikaite $\delta^{13}C$ values span a broad range, from < -30 to >-20 ‰, reflecting both organic matter and methane sources (Fig. 8; Jansen et al., 1987; Zabel and Schultz, 2001; Stein and Smith, 1986; Suess et al., 1982).

5. Conclusions

This study advances the existing model for ikaite to glendonite transformation, explaining the observations of etched boundaries and the different fabrics observed between the macro-zoned glendonites of the Kikutodden Member and the unzoned glendonites of the Carolinefjellet Formation. We explain the different fabrics observed between the Rurikfjellet Formation and Carolinefjellet Formation glendonites by the difference in sedimentation rates: the low sedimentation rates in the upper Rurikfjellet Formation meant that the ikaite/glendonite sat in the sulphate reduction zone for longer, such that the transformation from ikaite to glendonite was gradual, with conditions oscillating between ikaite stability and instability, resulting in the macro-zoned fabrics observed in the glendonites. Those of the Carolinefjellet Formation underwent rapid transformation from ikaite to glendonite, owing to elevated sedimentation rates causing the ikaite/glendonite to move out of the sulphate reduction zone (where ikaite is metastable) more quickly.

This new study highlights why ancient bulk glendonite $\delta^{18}O$ values cannot be used for palaeotemperature reconstructions, and has significant implications for using glendonites as quantitative palaeothermometers: if microsampling could be carried out such that only the "primary" calcite phase (Type I) were sampled, this could then be used for $\delta^{18}O$ or clumped isotope palaeothermometry, reintroducing glendonites as a palaeothermometry tool.

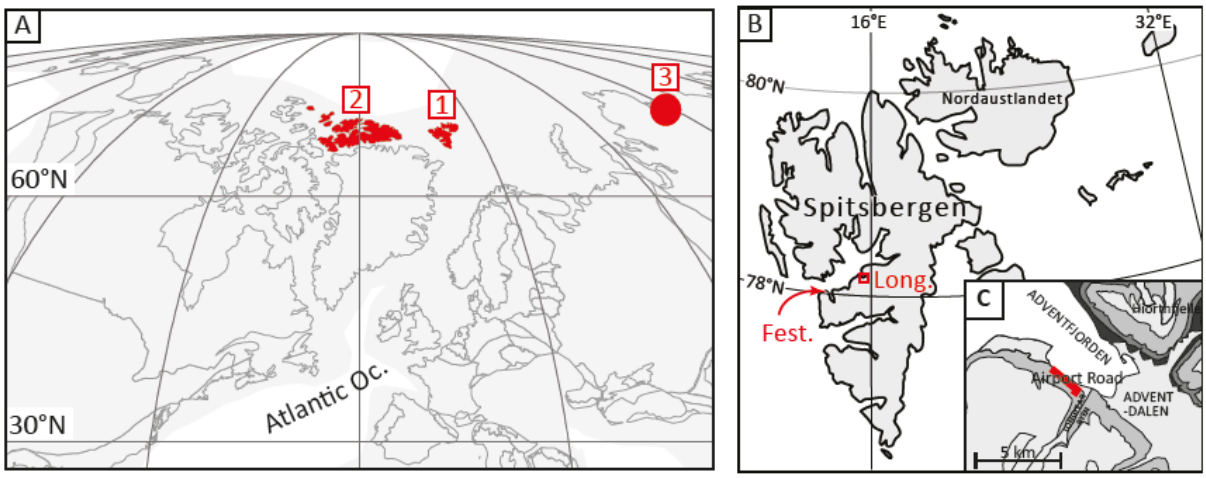

Figure 1: (A) Early Cretaceous paleogeography for the northern hemisphere, taken from Boucot et al. (2013); 1 = Svalbard archipelago; 2 = Queen Elizabeth Islands; 3 = northern Russian glendonite sites. **(B)** Location of sites studied on Svalbard. Long. = Longyearbyen; Fest. = Festningen. (C) Geological map of area around Longyearbyen, re-drawn from Major et al. (2000). Yellow = Paleocene – Eocene Van Mijenfjorden Group; light green = Carolinefjellet Formation; dark green = Helvetiafjellet Formation; blue = Rurikfjellet Formation.

Table 1. Descriptions of the glendonite horizons identified in this study, along with descriptions of the glendonites found in each horizon.

Sample ID	Horizon	Host lithology	Shape	Size (cm)	Structure	Comments
FST408–FST409	Festningen 408–409 m	Siltstone	Rosette	1–2	Macrozoned	Top (weathered) surface rust coloured, 'spider-web' pattern
FST411–FST412	Festningen 411–412 m	Siltstone	Cylindrical rosette	2–3.5 diameter 1–2.5 thickness	Macrozoned	Top (weathered) surface rust coloured, 'spider-web' pattern
FST441–FST442	Festningen 441–442 m	Siltstone	Partial rosette, Rosette	4–5	Macrozoned	
FST655	Festningen 655 m	Hummocky cross-stratified sandstone	Rosette	1.5–5	Rim and core, no macro-zoning	Range of size and shape. Smaller ones are 1.5 cm, flattened.
FST699.5	Festningen 699.5 m	Heterolithic siltstone-sandstone	Rosette (flattened)	1–2 x 0.5–1	Not zoned, poss. core	Rust-coloured weathered surface. Displacive growth in sediment pile.
FST708.5	Festningen 708.5 m	Heterolithic siltstone-sandstone	Rosette (flattened)	2.5–3.5	Zoned	
FST724.5	Festningen 724.5 m	Hummocky cross-stratified sandstone	Rosette	0.5–1	Not zoned	Beige; in darker host sed. 'coarse' appearance compared to host sed.
FST740	Festningen 740 m	Siltstone-sandstone	Cylindrical, not rosette form	2 x 2 x 1	Totally homogeneous	*May not be glendonite horizon; does not resemble other glendonites.*
FST753	Festningen 753 m	Siltstone	Rosette (flattened)	4.5 x 3	Core &/or rim	
APT2.1–APT2.5	Airport Road Lower 2–2.5 m	Siltstone-sandstone	Rosettes, cylindrical rosettes, partial rosette	3–4 rosette 2–4 blades	Core &/or rim	Pyritised cores in ones within cylindrical nodules
ABS22	Airport Road Upper 118–119 m	Siltstone-sandstone	Rosettes, partial rosettes, blades	3–4 rosette 2–3 blades	Not zoned	v. lumpy, shape indistinct, often broken/in bits

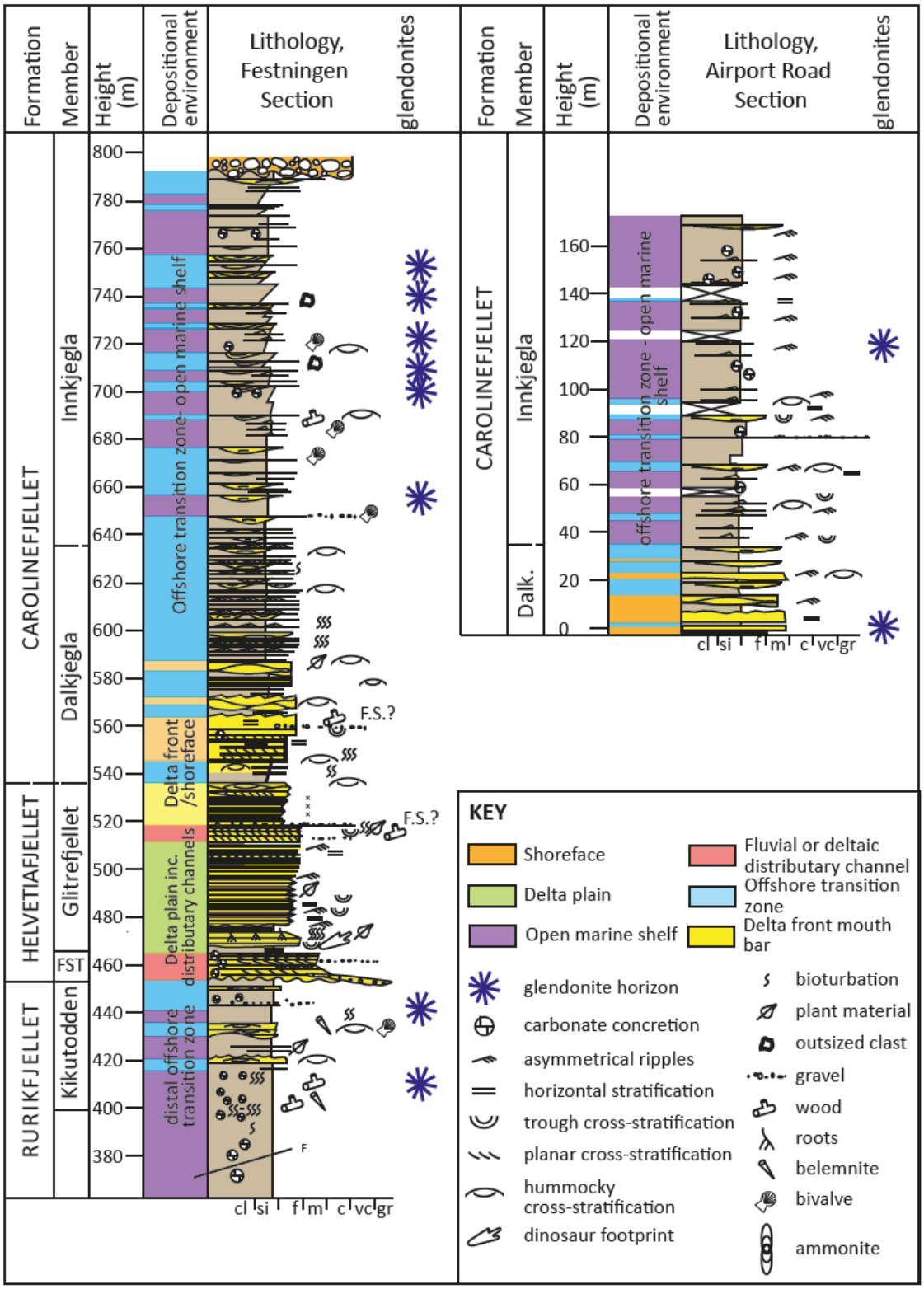

Figure 2: Sedimentary location of glendonites in Festningen and Longyearbyen localities. Festningen log modified after Vickers et al., 2016. Lithostratigraphy, facies associations and interpreted depositional environments also shown. FST=Festningen Member; Dalk. = Dalkjegla

Member. F.S.=Flooding Surface.

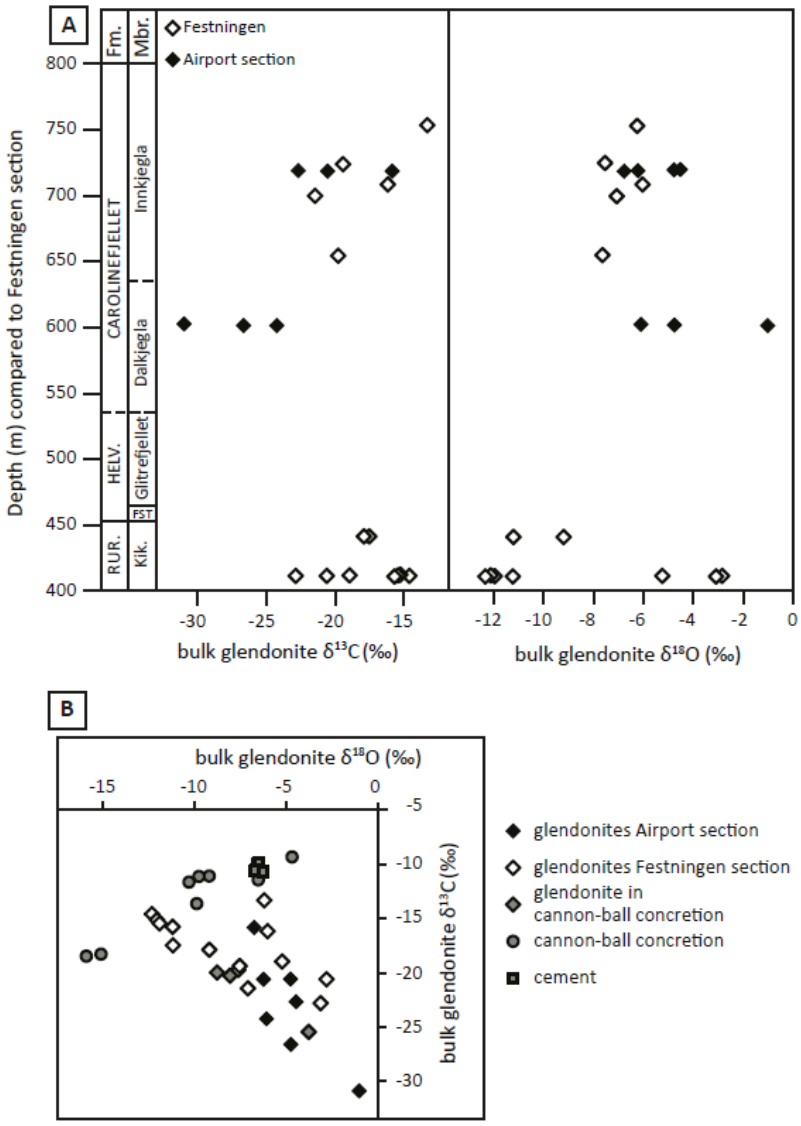

Figure 3: (A) Bulk glendonite $\delta^{13}C$ and $\delta^{18}O$ results plotted against stratigraphic height in the Festningen section. Glendonites from Airport Road section are shown in black diamonds, using the chemostratigraphic and sequence stratigraphic correlation to the Festningen section of Vickers (2017). **(B)** Bulk glendonite $\delta^{18}O$ plotted against bulk glendonite $\delta^{13}C$ for glendonites from the Festningen section (white diamonds) and Airport Road section (black diamonds). $\delta^{13}C$ and $\delta^{18}O$ data for a glendonite in a carbonate (cannon-ball) concretion, along with data for the concretionary calcite and matrix, shown in grey (diamonds, circles and squares, respectively). The negative correlation between $\delta^{13}C$ and $\delta^{18}O$ for the glendonites is clear.

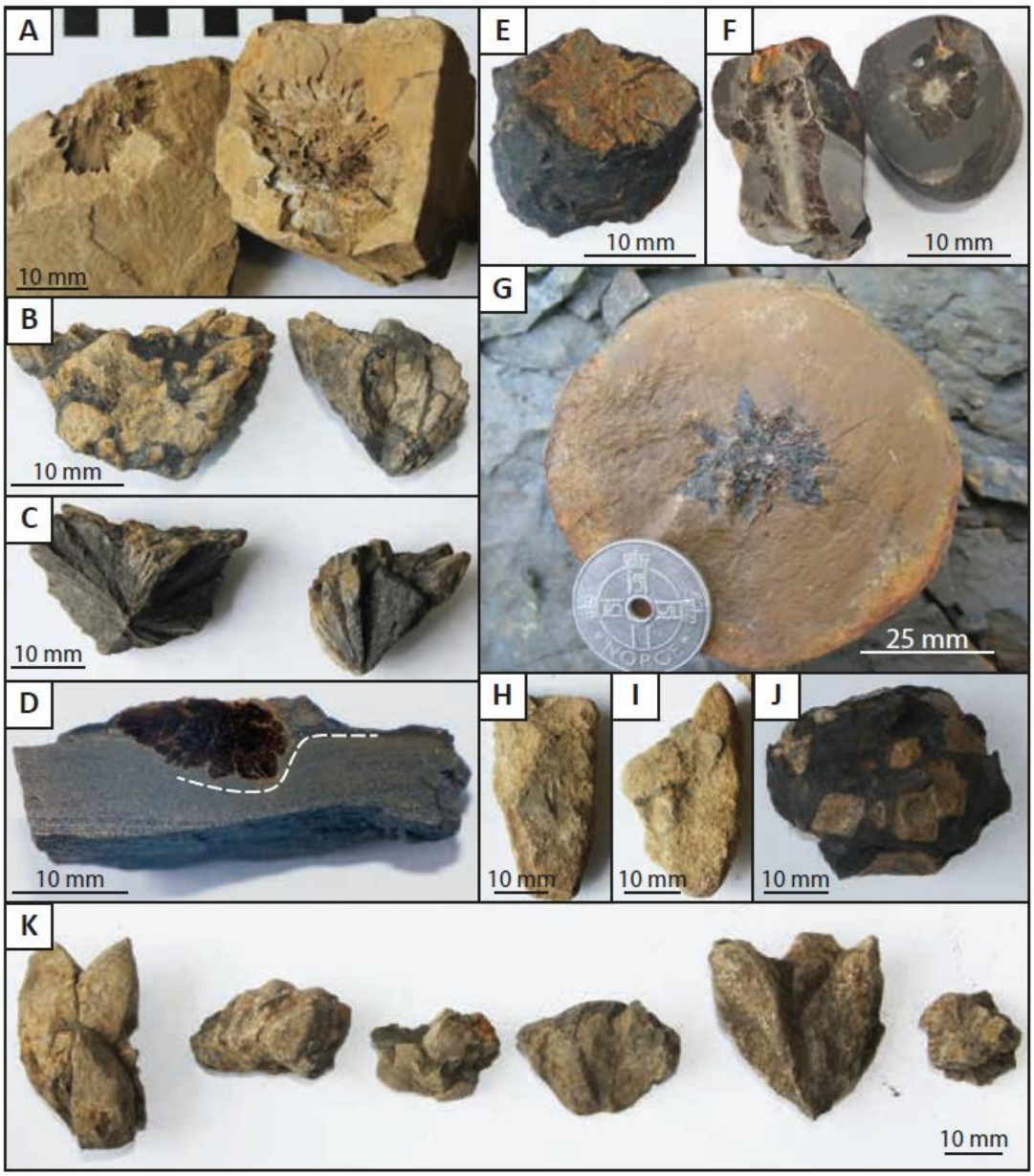

Figure 4: Range of shapes of glendonites sampled from Festningen and Longyearbyen. Scale: black and white cubes = 5 mm each; black bars on blue background = 1 mm between bars. **(A)** Rosette form glendonite from 655 m in the Festningen section; poor preservation. **(B)** and **(C)** Partial rosette glendonites from the Festningen section, horizon 441.25 m (photographs of opposite sides of the glendonites); mm-scale zoning just visible. **(D)** Flattened rosette form glendonite from 699.5 m in the Festningen section. Sediment distorted around glendonite. **(E)** Glendonites from 2.2 m in the Airport road section; partial rosette forms. **(F)** Festningen, glendonite horizon at 411.6 m; cylindrical rosette form. **(G)** Cylindrical rosette glendonites inside concretion, with distinct pyritised core, from 2.2 m in the Airport road section. **(H)** Rosette glendonite inside concretion. **(I)** and **(J)** Bladed glendonites from the Airport Road section, horizon at 118 – 119 m, blades. **(K)** Rosette glendonites from horizon at 118 – 119 m of the airport road section.

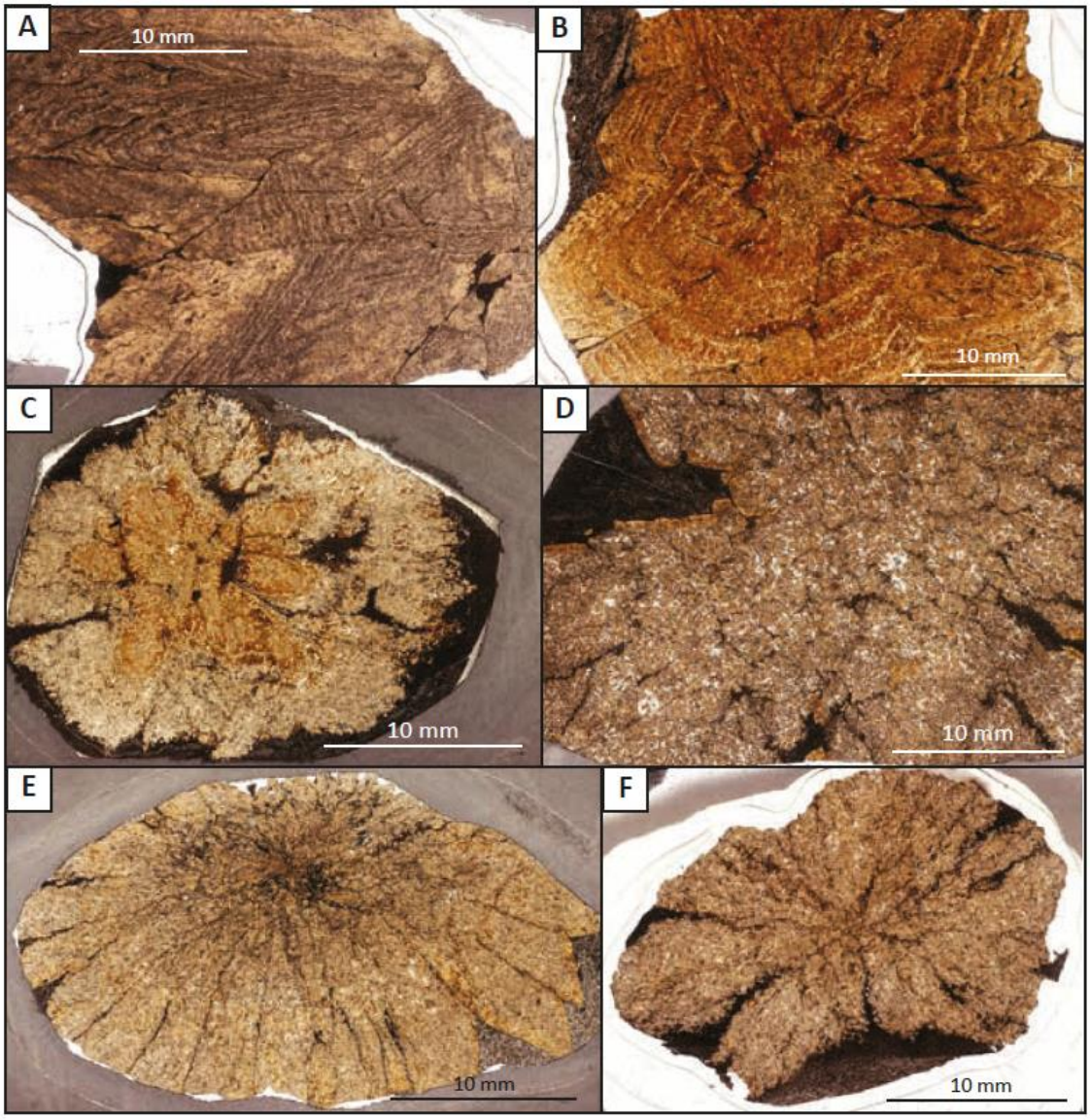

Figure 5: Photographs of thin sections showing their internal structure (zoned, core/rim, unzoned). **(A)** Macro-zoned glendonite from 441.25 m in the Festningen section. **(B)** Macro- zoned glendonite from 411.5 m in the Festningen section. **(C)** Glendonite with distinct core from 2.2 m in the Airport Road section. **(D)** Glendonite from 753.15 m in the Festningen section, showing a narrow rim, inside unzoned. High percentage of clear calcite spar. **(E)** Unzoned flattened rosette glendonite from 655 m in the Festningen section. **(F)** Glendonite from 118 - 119 m in the Airport Road section core slightly distinct for rest of glendonite.

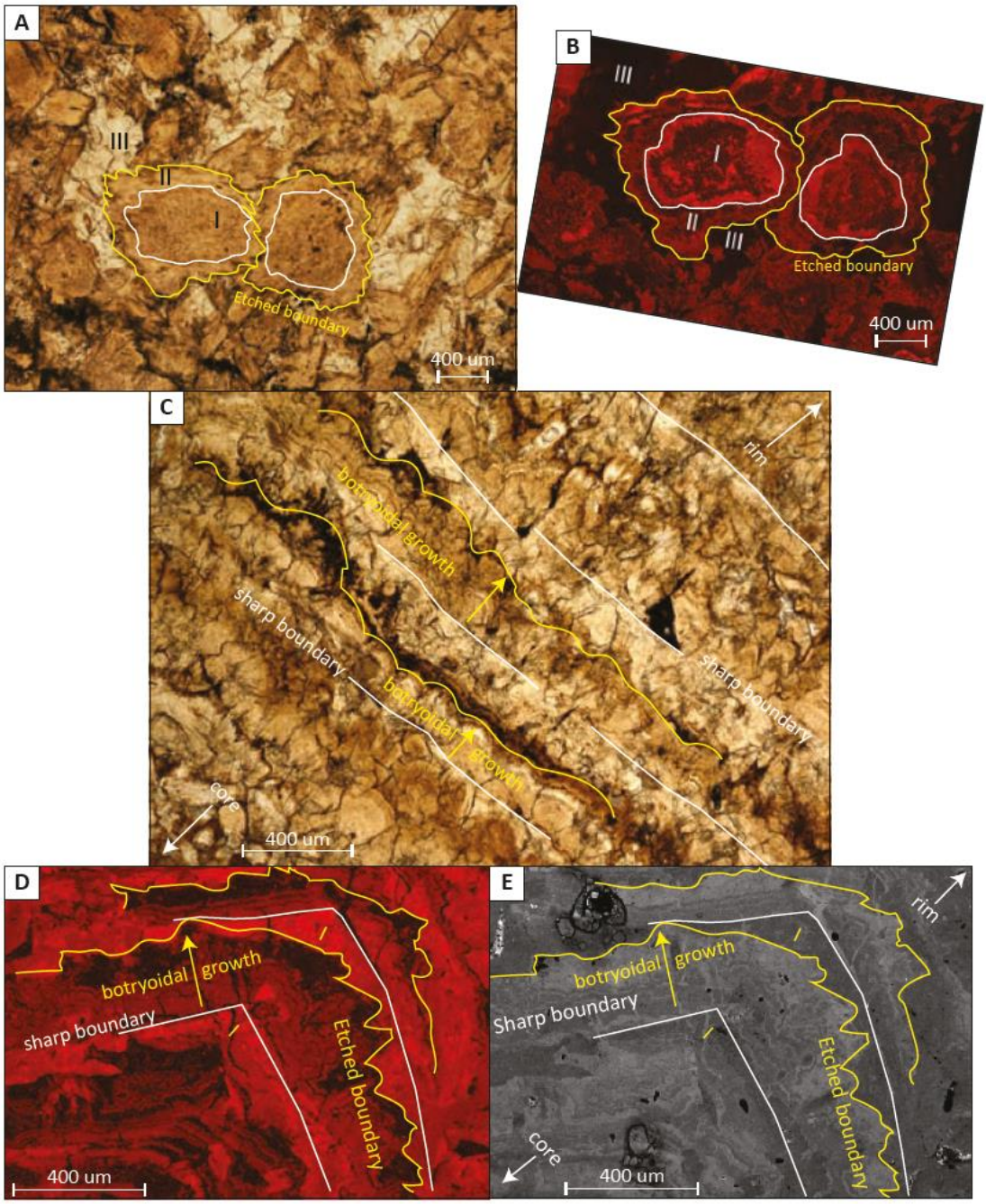

Figure 6: Microzonation in glendonites. White outline around primary ikaite-derived calcite (I); yellow outline around secondary calcite (II). Final phase of calcite growth (clear spar) labelled "III". **(A)** Thin section of an "unzoned" (not showing macro- zonations) glendonite (755 m, Festningen) under plane polarised light. **(B)** CL photomicrograph of the same glendonite thin section. Micro-zonation very clear. **(C)** Thin section of a macro-zoned glendonite under plane polarised light (411.5 m, Festningen). Sharp planar surfaces with botryoidal growth of secondary calcite. This suggests that the botryoidal phase always nucleated on a planar surface. **(D)** Thin section of macro-zoned glendonite (441.25 m, Festningen) under CL. Darker = higher iron; indicating increasing iron content of calcite as the secondary botryoidal calcite grew. **(E)** SEM image of the same glendonite.

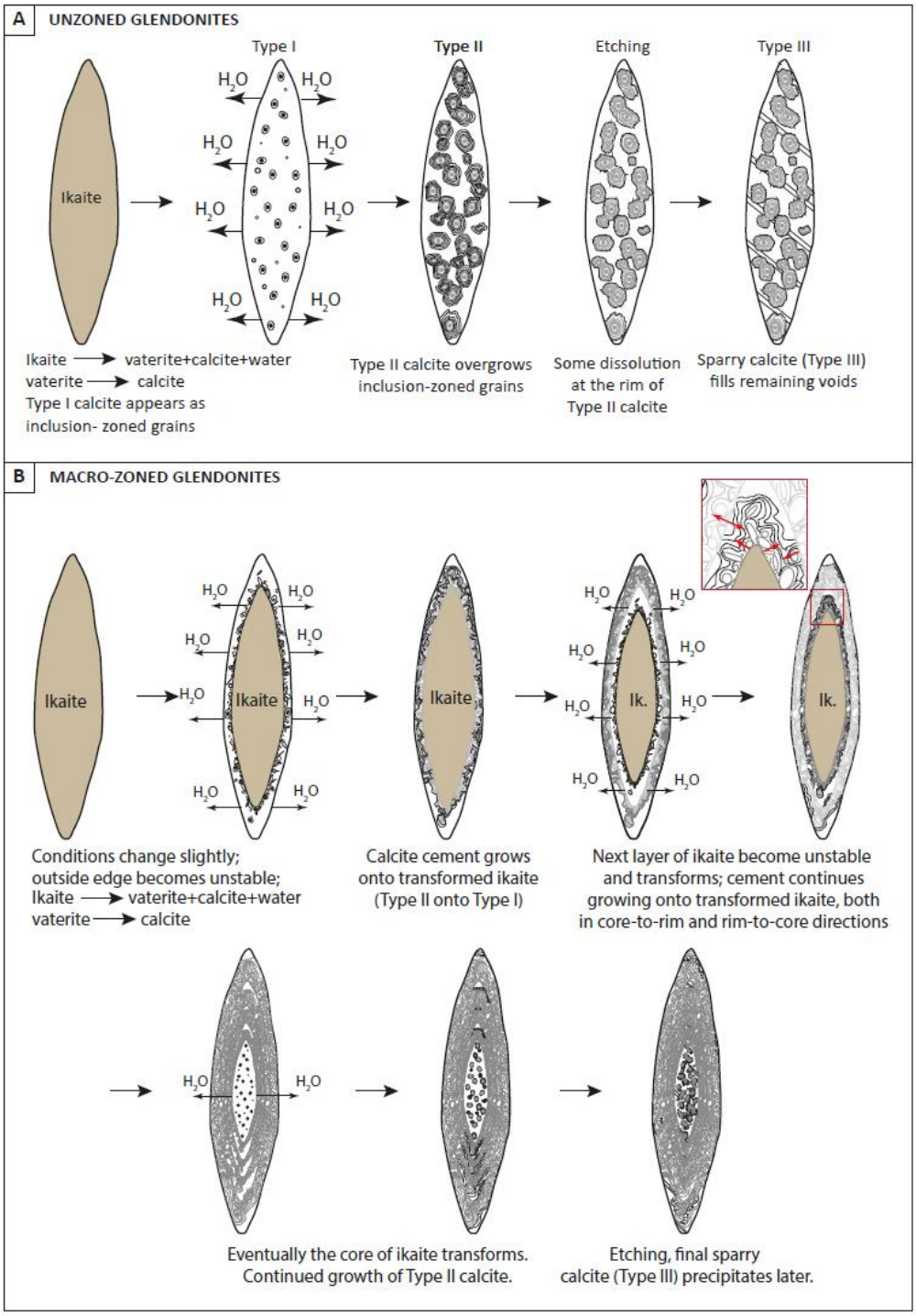

Figure 7: Models for ikaite-to-glendonite transformation, modified after Teichert and Luppold (2013) and Frank et al. (2008a). **(A)** Model for ikaite-to-glendonite transformation for unzoned glendonites, whereby ikaite breaks down to a mix of vaterite, calcite and water, and the vaterite rapidly transforms to calcite. This transformed ikaite-calcite is still sitting in the sulphate reduction zone, and experiences rapid diagenetic calcite overgrowth. This ceases when the sediments in which it lies move out of the sulphate reduction zone, and partial dissolution may occur at the edges of the diagenetic calcite. An unknown amount of time later, late-stage sparry calcite infills any voids. **(B)** Model for ikaite-to- glendonite transformation for macro-zoned glendonites, whereby oscillations in conditions resulting in the slow, progressive breakdown of the ikaite crystal, from the outside in.

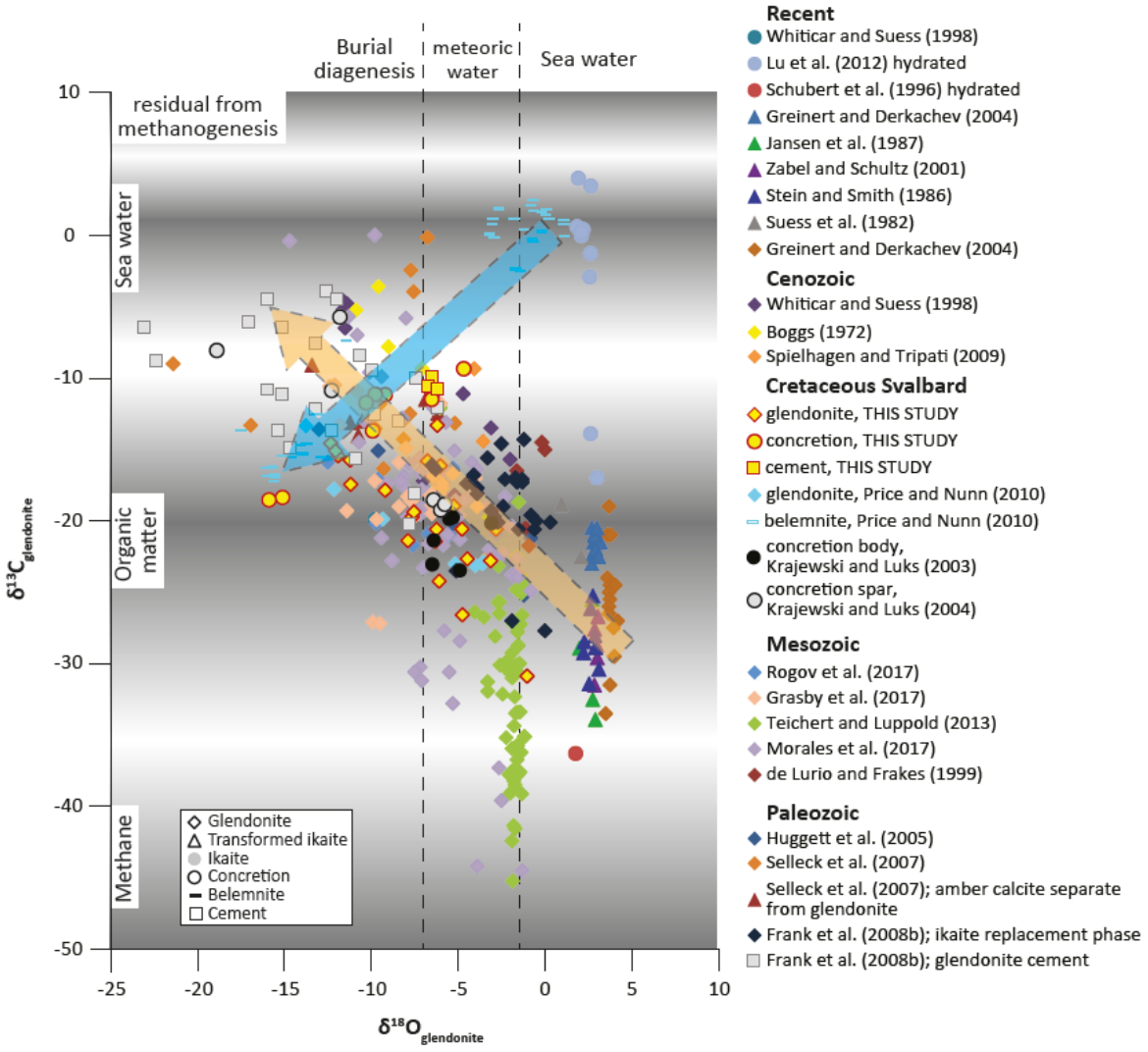

Figure 8: Glendonite and concretionary calcite stable isotope data gathered in this study compared to Svalbard belemnite calcite (Price and Nunn, 2010), Svalbard cannon-ball concretion (Krajewsky and Luks, 2004), glendonite, transformed ikaite and ikaite $\delta^{13}C$ and $\delta^{18}O$ data from previous studies (sources cited on figure). The $\delta^{13}C$ ranges for methane, organic carbon and sea-water (as given by Campbell, 2006) are indicated by grey shading. The $\delta^{18}O$ ranges for sea-water, meteoric water, and those associated with burial diagenesis (as discussed in Campbell, 2006), are indicated by dashed lines. Blue arrow indicates evolutionary trends for typical meteoric diagenesis (heavy $\delta^{13}C$ and $\delta^{18}O$ to light $\delta^{13}C$ and light $\delta^{18}O$ with increasing burial depth and diagenetic alteration); beige arrow shows sulphate reduction zone evolutionary trends from light $\delta^{13}C$ and heavy $\delta^{18}O$ to heavier $\delta^{13}C$ and lighter $\delta^{18}O$.